Circulation Controlled STOL Wing Optimization

John L. Loth* and Michael Boasson†
West Virginia University, Morgantown, West Virginia

By replacing the sharp trailing edge of an airfoil with a rounded Coanda surface, one can generate high lift at a moderate blowing rate. In such a circulation controlled (CC) airfoil, a two-dimensional wall jet is used to force the rear stagnation point down and increase the circulation and lift. The CC airfoil performance and blowing power requirements depend on both the wall jet momentum and the wall jet to freestream velocity ratio because a significant portion of the wall jet momentum is lost to shear over the Coanda surface. When using high-pressure jet engine bleed air, an internal wall jet ejector can be used to optimize the wall jet velocity. This will reduce the required bleed airflow rate and cool the wing structure, in addition to providing boundary-layer control by suction. The applicability of CC high lift generation for short takeoff and landing aircraft was first demonstrated at West Virginia University in April 1974 with the WVU CC Technology Demonstrator STOL Aircraft. A second such CC technology demonstrator, a modified Navy A-6A was test flown five years later. The importance of optimizing the wall jet velocity is analyzed in this paper.

Nomenclature

A = nozzle to exit area ratio for a constant area ejector
c = cruise chord length
C_D = drag coefficient
C_f = wall jet skin friction coefficient
C_L = lift coefficient based on cruise chord
$C_{L,0}$ = lift coefficient at $\alpha = 0$ and $C_\mu = 0$
ΔC_L = lift increase due to blowing
$C_{L_{max}}$ = maximum lift coefficient
ΔC_n = force coefficient normal to a flat plate
C_Q = dimensionless average suction velocity
$\bar{C}_\mu$ = wing area momentum coefficient based on total mass flow rate
C_μ = two-dimensional airfoil momentum coefficient
C_{μ_j} = C_μ of the ejector exit momentum
C_{μ_n} = C_μ of nozzle without an ejector
D = drag force
f = fraction of wall jet momentum lost to wall shear
h = wall jet height
L = lift force
$\dot{m}_b$ = mass flow rate inside boundary layer
$\dot{m}_j$ = mass flow rate in the wall jet from ejector exit
$\dot{m}_n$ = ejector nozzle mass flow rate
$\dot{m}_s$ = boundary-layer suction mass flow rate equal to the ejector secondary flow
p_∞ = ambient pressure
P_B = blowing power
P_T = thrust power
Re_c = Reynolds number based on chord
Re_j = Reynolds number based on distance downstream of wall jet
S_w = wing area
V_i = indicated airspeed
V_{EW} = airspeed reduced to sea level and gross weight
V_j = wall jet velocity when fully expanded to p_∞
V_n = ejector nozzle velocity when fully expanded to p_∞
V_∞ = free-flight velocity
α = angle of attack
β = flap deflection angle
δ = boundary-layer thickness
δ^* = boundary-layer displacement thickness
δ_e^0 = stabilator angle in degrees
ρ = density
ν = kinematic viscosity

Presented as Paper 83-0082 at the AIAA 21st Aerospace Sciences Meeting, Reno, Nev., Jan. 10-13, 1983; received Jan. 28, 1983; revision received July 22, 1983.

*Professor, Mechanical and Aerospace Engineering. Member AIAA.
†Instructor, Mechanical and Aerospace Engineering.

Introduction

SHORT takeoff and landing (STOL) aircraft find applications in both commercial and military operations. They can take off and land on runways less than 600 m (2000 ft) long and have descent and climb angles several times greater than those of conventional aircraft. This gives them a good obstacle clearance capability and a small noise footprint on the suburban area surrounding the airport. STOL capability is very desirable for aircraft landing on a rolling and heaving deck of a carrier. The risk of an accident can be significantly reduced by lowering the approach speed. The advantages of STOL capability are partially offset by the extra complexity, weight, cost, and power required. The necessary pilot skill and work load for STOL further limits its application.

The most impressive STOL performance is obtained when the aircraft has a high thrust to weight ratio. The STOL wing must have high lift coefficient (C_L) capability, and the wing area should be increased in the STOL mode to reduce the wing loading and associated stall speed. One of the most important requirements for a STOL aircraft is its capability to convert the wing in flight, from a high lift configuration to one with low drag for high speed. This is needed for good climb and cruise performance, in addition to STOL capability. High jet engine bleed air requirements for powered lift generation will produce a significant thrust loss. This may offset the advantage of the lower takeoff speed, which is intended to reduce the minimum runway length.

The design of an optimum configuration of a powered high lift wing involves a careful tradeoff of obtainable lift as a function of required blowing power from the available compressed air source. The associated aircraft handling qualities on takeoff, climb, conversion for high lift to cruise and back, during the approach, flare-out, and landing must all be considered in this design tradeoff.

STOL Wing Aerodynamics

In the STOL mode, the pilot operates on the backside of the power curve, and his workload is high. On complicated STOL aircraft it may be necessary to consolidate the pilot controls into a single descent control lever. Its input is fed into a computer, which in turn controls the throttle, elevators, flaps,

high lift devices, and wing leveler. When using a short runway, the touchdown area is very restricted. As a result, the glide slope corridor is narrow in addition to being steep. To stay on such a narrow glide path, the pilot needs a direct lift control system (DLC). The use of DLC allows the descent rate to be altered without changing the aircraft attitude and thus the speed. To maintain good pilot visibility, the aircraft's wing should be able to generate a high C_L in a near level flight attitude. Another problem of low-speed flight is the aircraft's gust sensitivity. To cope with this, the effectiveness of the control surfaces may need to be augmented by using blown ailerons and an empennage embedded in the engine exhaust flow.

At high C_L operation, by using either jet blowing or thrust deflection, the touchdown procedure requires special pilot skills. On conventional aircraft the flare-out is initiated by back pressure on the control stick. The resulting nose-up attitude increases the wing angle of attack and, proportionally, the lift produced. The relative increase in lift produced determines the radius of curvature of the flare-out maneuver. However, in the powered lift STOL mode, most of the wing lift is generated independently of the angle of attack. Thus back pressure on the stick, which results in an increase of the aircraft's attitude and angle of attack, has little effect on the relative lift increase. Thus the flare-out has to be sacrificed, resulting in a hard landing unless a reserve of lift generating blowing power is available for flare-out.

STOL aircraft wings can be classified into four groups by the power required for high lift generation:

1) Unpowered high lift generation by using special flaps and leading edge modifications

2) Low power requiring high lift generation employing boundary-layer control (BLC) by suction or blowing. Here the wing lift coefficient is only a function of the angle of attack and flap deflection. Often the pilot visibility is reduced during approach, when using a high angle of attack.

3) Medium power requiring high lift generation by circulation control (CC). This technique uses a two-dimensional wall jet to blow over a rounded Coanda surface. The wall jet turning forces the rear stagnation point down to create circulation and high lift. Boundary-layer separation criteria control the location of the rear stagnation point and the resulting lift coefficient. CC blowing produces a higher ratio of lift augmentation over blowing momentum than others, such as jet flap, the blown flap, or the augmenter wing. The obtainable lift coefficient of the latter devices depends on the extent to which the jet is deflected downward.

4) High power requiring lift generation by engine thrust deflection. A significant portion of the deflected engine exhaust momentum is recovered as thrust in the form of wing leading edge suction.

Some typical wing configurations in these four categories are shown in Fig. 1. All have their particular advantages and limitations, which are well described by Kohlman.[1] The borderline between low, medium, and high power required cannot be clearly defined. An insight into the division of these groups can be obtained by considering the power required for high lift generation relative to the thrust power required for level flight. Consider blowing air with a mass flow rate $\dot{m}_j$ and jet velocity V_j. The blowing momentum is assumed to be fully recovered in the form of thrust. The relative blowing power required is the ratio of the kinetic blowing power to the thrust power. The thrust equals the drag D minus the recovered jet momentum $\dot{m}_j V_j$:

$$\frac{P_B}{P_T} = \frac{\dot{m}_j V_j^2/2}{V_\infty (D - \dot{m}_j V_j)} \tag{1}$$

where the subscripts B and T stand for the blowing and thrust power, respectively.

Defining C_μ as the average wing blowing coefficient based on the projected cruise wing area S_W, with flap stowed,

$$\bar{C}_\mu = \frac{\dot{m}_j V_j}{\tfrac{1}{2}\rho V_\infty^2 S_w} \tag{2}$$

Note C_μ is used for a two-dimensional wing. The power ratio becomes

$$\frac{P_B}{P_T} = \frac{V_j}{2V_\infty} \Big/ \left(\frac{C_D}{\bar{C}_\mu} - 1\right) = \frac{V_j}{2V_\infty} \Big/ \left(\frac{C_L}{\bar{C}_\mu} \cdot \frac{D}{L} - 1\right) \tag{3}$$

This power ratio shows that the blowing power required increases with $\bar{C}_\mu$ and is proportional to the velocity ratio (V_j/V_∞). The contribution of the ratio $(C_L/\bar{C}_\mu)$ to the blowing power required is quite different for the various high lift systems; this is shown in Fig. 1, from Ref. 2.

The lowest power requiring high lift airfoil employs boundary-layer control (BLC) by blowing at $C_\mu < 0.02$ or by suction with $C_Q < 0.004$. It's effect is mainly to delay stall and thereby increase $C_{L_{\max}}$; therefore it results in a high augmentation ratio $(\bar{C}_L/\bar{C}_\mu)$. An extensive analysis of the potential of boundary-layer control by suction was done by Pfenniger.[3] Suction not only permits very high angles of attack and high $C_{L_{\max}}$ but also significantly lowers the drag by laminarization of the boundary layer. Very impressive STOL performance was obtained with the MK-4 aircraft tested at the University of Cambridge, England. With a suction coefficient $C_Q = 0.004$, it could fly at 33 knots with 45-deg angle of attack.

The research team at Mississippi State University has constructed and tested several light aircraft with BLC, for which the suction power required was less than 20 hp. The team members developed a variable camber wing to overcome the problem of poor pilot visibility at high angles of attack. Although the lower power requirements appear very attractive, the structural and operational problems associated with numerous small suction holes limit its applicability. Another efficient form of BLC and high lift generation is to energize the boundary layer by moderate blowing at $C_\mu < 0.02$. This technique is described by Katzmayer.[4] With BLC it is only the angle of attack of the airfoil and flap which controls the circulation and lift on the airfoil.

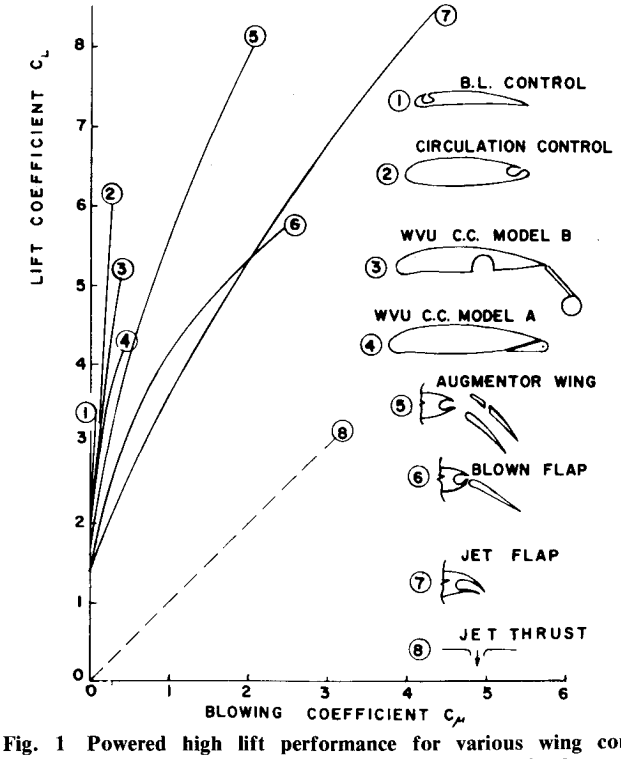

Fig. 1 Powered high lift performance for various wing configurations; the lift augmentation ratio is proportional to the slope.

The method of high lift generation by circulation control at $C_\mu < 0.4$ has a lower power efficiency factor than BLC, but has many STOL operational advantages that will be discussed later.

The other methods of high lift generation have even lower power efficiency factors. However, this disadvantage can be entirely offset by their thrust recovering ability. Examples are the augmenter wing, the over surface blowing, and the jet flap. The highest power will be required by a simple jet thrust lift system without thrust augmentation. Such a jet thruster has an augmentation ratio $C_L/\bar{C}_\mu = 1.0$. At high values of $\bar{C}_\mu$, the jet momentum makes a significant contribution to the thrust.

The jet, after leaving a two-dimensional airfoil surface, is ultimately turned back in the freestream direction. Thus its momentum can be recovered in the form of thrust. This was proven by Spence[5] for the jet flap. The thrust recovery limitations caused by the effects of downwash on finite wings are described by McCormick.[6] The thrust recovery aspects for the augmenter wing are discussed by Wilson[7] and further elaborated upon by Bevilaqua.[8] The downward deflected jet makes a curved path such that the centrifugal force on the curved jet is kept in balance by the external flow pressure difference across the jet. The downwind component of the jet wake surface pressure force in the direction of V_∞ contributes to the thrust recovery in the form of leading edge suction on the airfoil. The remainder of the jet momentum thrust contribution is the downwind component of the jet momentum at the airfoil exit. Only a two-dimensional airfoil has no downwash and the combined effect of these two thrust contributions are equal to the total momentum of the jet. The pressure difference on the jet wake can also be represented by a vorticity. This starts with a finite value at the airfoil jet exit and reduces to zero as the jet turns in the direction of the flight velocity. This creates a finite loading at the trailing edge of the airfoil and provides the boundary condition required to compute the lift contribution from the deflected jet wake.

In high lift systems using circulation control or the blown flap, the jet does not leave the airfoil surface immediately. During its trajectory as a wall jet, a significant portion of its momentum is lost by wall shear and is not recoverable as thrust. This is especially true when the wall jet path length is long compared to the initial jet thickness, or when C_μ is small or V_j/V_∞ is high. The radial pressure gradient in the curved wall jet creates a low-pressure on the surface. This allows the jet to remain attached to the rounded trailing surface through a Coanda[9] turning ability into the adverse pressure gradient created by the flow passing underneath the airfoil.

The originator of circulation control high lift generation was Davidson.[10] Experiments on an elliptical airfoil were carried out by Kind[11] at Cambridge University. Kind developed the first analytical treatment of the wall jet on a Coanda surface of an elliptic airfoil. The impressive performance capability of circulation control encouraged the Office of Naval Research (ONR) to sponsor further research. Circulation control high lift generation does not have the operational problems associated with BLC by suction through many small holes. Small holes can easily clog with dirt, rain, or ice, which may produce unreliable high lift characteristics. The Navy developed the elliptical airfoils with CC for use in high lift and high speed helicopter blades, with leading edge (LE) and trailing edge (TE) reversal capability. This research was pursued by Williams[12] at the Naval Ship Research and Development Center (NSRDC). His contribution resulted in the construction of the XH2 CCR Circulation Controlled Helicopter. Concurrently at West Virginia University, Walters and others conducted wind tunnel experiments on CC elliptical airfoils. Gibbs and Ness[13] developed a computer program that calculates the circulation controlled elliptical airfoil performance characteristics. They are a function of geometry, angle of attack, C_μ, V_j/V_∞, Re, and, in particular, the boundary-layer profile shape parameter upstream of the wall jet. The numerical boundary-layer analysis uses as input the pressure field from the external potential flow.

In 1970, the wind tunnel experiments at NSRDC and at WVU indicated the high-performance sensitivity to the geometry of the aft 5% of the airfoil. Also, the Reynolds number and the wind tunnel wall interference all had a major influence on the measured power efficiency. To clarify some of these parameters, a large-scale, high Reynolds number free-flight test was proposed by WVU in 1970. It was just as easy to change the wings on the aircraft to CC airfoils as to add a separate test CC airfoil to the conventional wings. This resulted in the design, construction, and, in 1974, the flight testing at WVU of the first Circulation Control Technology Demonstrator Aircraft, see Fig. 2. The elliptic airfoil was not suitable for STOL flight operations, and a standard NACA 64_2-415 airfoil was selected for CC modification.[2] In 1971, the first model A wing was designed and constructed. It featured an in-flight conversion from a conventional sharp trailing edge flap to a high lift rounded trailing surface with Coanda blowing, by folding the flap fully forward in a cavity provided for it. Blowing with low-pressure air was feasible even in the blown flap configuration at all flap angles. Model A is shown in Fig. 1 with the flap folded forward and stowed in the circulation control configuration. The drooped leading edge with blowing slot was designed by Dr. Norio Inumaru, visiting WVU from NRL in Tokyo. The 4-ft chord and 8-ft span model A wing constructed at WVU was tested in the NSRDC wind tunnel. The test results can be summarized as follows:

1) The pitching moments associated with folding the flap forward and stowing it are acceptable.

2) With blowing, the lift coefficient, based on the cruise chord, increased after the flap was folded and stowed; thus the CC configuration performed better than the blown flap configuration.

3) In the CC configuration, the chord length should be increased instead of decreased by 12%, as it was in model A.

4) Low-pressure air wall jet blowing uniformity is difficult to achieve and high-pressure air ducting is recommended.

5) The drooped leading edge design was capable of preventing leading edge stall, even without LE blowing. All

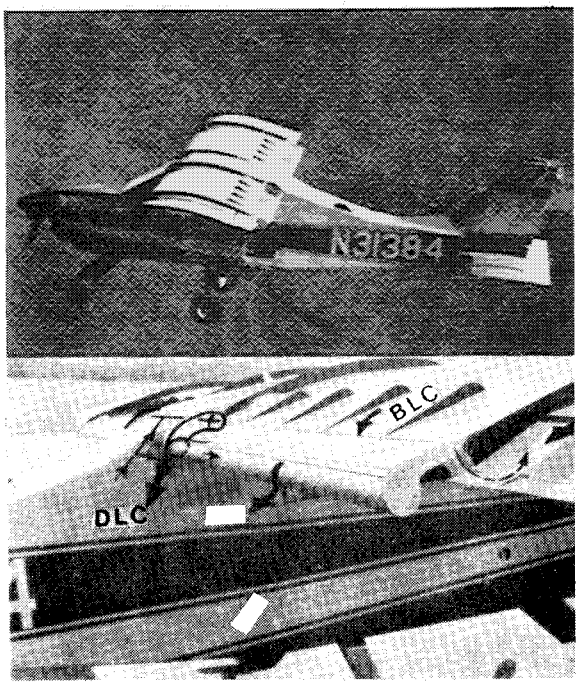

Fig. 2 The first circulation control technology demonstrator STOL Aircraft with CC flap deployed. Insert shows blowing air path and outlets.

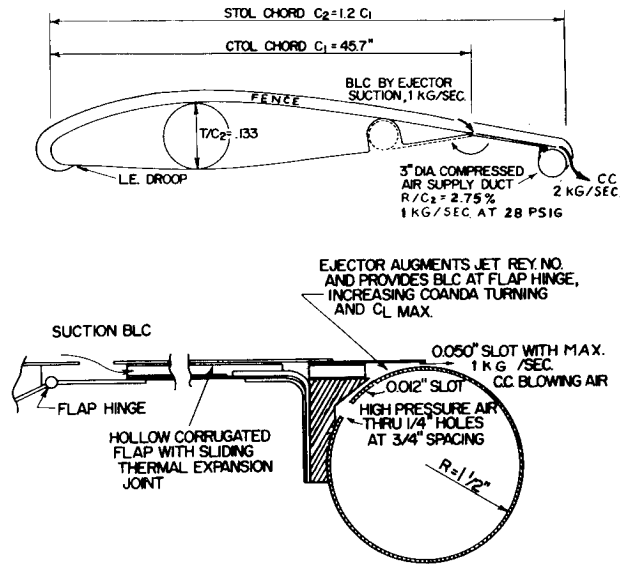

Fig. 3 The WVU Technology Demonstrator Aircraft model B STOL wing design with forward folding, stowable flap.

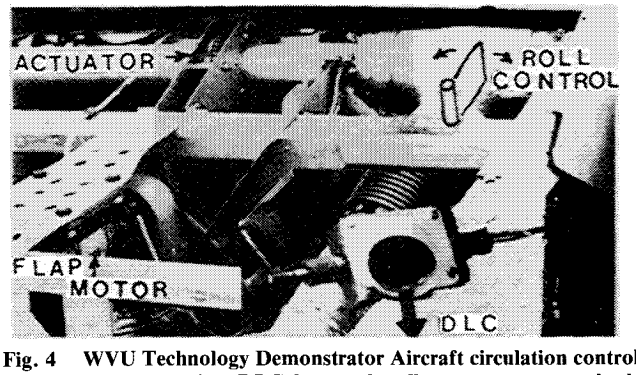

Fig. 4 WVU Technology Demonstrator Aircraft circulation control air supply ducts showing: DLC dump valve, flap actuator wormwheel, and air diverter valve for roll control by differential blowing.

tests were run at constant wall jet slot height ratio h/c and ΔC_L increases linearly with the wall jet velocity or with the square root of the momentum coefficient ($\sqrt{C_\mu}$),

$$C_L = C_{L,0} + \alpha\left(\frac{\partial C_L}{\partial \alpha}\right) + C_\mu\left(\frac{\partial C_L}{\partial C_\mu}\right) \tag{4}$$

For the model A wind tunnel test, it was found that

$$\frac{\partial C_L}{\partial \alpha} = 5.0 \text{ (per rad)} \quad \text{and} \quad \frac{\partial C_L}{\partial C_\mu} = \frac{3.5}{\sqrt{C_\mu}}$$

Note that the coefficients are referenced to the larger cruise chord.

From the experience gained with the model A wing, the model B wing was designed and wind tunnel tested at WVU, see Fig. 3. The in-flight conversion, from a high lift CC configuration to a low drag sharp TE was improved. A normally stowed flap with a rounded trailing surface was folded outward and thus increased the chord by 20% in the CC mode. The low-pressure air duct was replaced with a high-pressure air duct. A saddle bolted to the tubular air supply duct was machined to form a close tolerance two-dimensional converging-diverging nozzle with a 0.3-mm (±5%) throat height. This supersonic nozzle supplies the primary air for an internal ejector with a 1.2-mm exit slot. The internal ejector is essential to reduce the ratio V_j/V_∞ for better Coanda turning. Because the blowing air tube operates at a high temperature (157°C), the ejector is also required to provide flap cooling. The suction air flowing through the hollow flap lowers the temperature of the structure near the fuel which is stored in the wing. An additional benefit of the internal ejector is that it removes the low-energy portion of the upstream boundary layer with a suction slot located at the flap hinge line. The leading edge nose radius was reduced to equal that of the CC rounded Coanda surface with a radius of 3.75 cm. The model B wind tunnel test data can be approximated by the same empirical equation. The tests were performed with a constant slot height to cruise chord ratio $h/c=0.001$ and $Re_c = 4.5\times10^5$.

$$\frac{\partial C_L}{\partial \alpha} = 5.5 \quad \text{and} \quad \frac{\partial C_L}{\partial C_\mu} = \frac{6.6}{\sqrt{C_\mu}}$$

In the wind tunnel model, the CC blowing airflow rate and the hinge line suction air were controlled individually. An ejector mass flow rate of $\dot{m}_{\text{suction}} = \frac{1}{2}\dot{m}_j$ could be maintained. The benefit of boundary-layer suction was measured by taping off the suction slot. For the tests with the flap straight out, the elimination of BLC by suction lowered C_L at all angles of attack. With the flap at 15 deg the elimination of suction caused a drop in $C_{L_{\max}}$ of 8%. This demonstrates the improvement obtainable in CC effectiveness when the boundary-layer shape factor is improved upstream of the Coanda wall jet. This is especially true when the external flow has to negotiate a turn at the flap hinge line.

The wind tunnel model B performance was found to be very satisfactory, and the same configuration was selected for full-scale flight testing. It was decided to build a Circulation Control Technology Demonstrator Aircraft using the basic structure from a BEDE 4 aircraft kit. By building the aircraft from the ground up, its design was not restricted. The technology demonstrator incorporates all the desired CC test features. A 180-hp Lycoming reciprocating engine was chosen to provide aircraft propulsive thrust, independent of the blowing system. A 200-hp GTC 85-72 gas turbine was placed in the back seat to provide up to 1 kg/s compressed air for CC blowing. At sea level, the available pressure in the CC supply air duct was 158 kPa (23 psig) at 157°C (250°F). The air supply could be entirely dumped through a sliding gate valve on linear roller bearings. The mixture control lever on the throttle quadrant was used to operate this dump valve for convenient direct lift control (DLC) by the pilot. Downstream of this dump valve the air enters a tee section supplying both wings, as shown in Fig. 4. Inside the tee section is a flow diverter valve, which is coupled to the normal aileron control system, with a linkage of adjustable ratio. This enables the pilot to use differential blowing at low flight speeds, to assist the ailerons in lateral control. This option has not yet been flight tested. In the fuselage, the supply duct had to be placed at the flap hinge centerline and had to serve as flap actuator. The supply duct is connected by a hollow crank to the 7½-cm-diam CC blowing tube. The hollow crank transmits the required torque to the flap. The flap is actuated by rotating the supply air duct with a 2-hp electric motor. The high-temperature trailing edge CC blowing tube was allowed to expand freely and is connected only to the hollow flap by a sliding slip joint. The hollow flap that transports the internal ejector suction air is fastened to the wing with a piano hinge. During operation, the CC blowing tube expanded more than 1 cm without altering the blowing slot height.

To improve the aerodynamic spanwise loading efficiency it was necessary to install four large fences on the wing, as shown in Fig. 2. The small fences shown serve only to connect structurally the flap assembly to the rigid structure near the main spar. They were required because the internal wing structure had to be eliminated at the location of the cavity, in which the CC blowing tube is stored in the cruise configuration. Five percent of the total blowing air was supplied

to each aileron for upper surface blowing. The aileron supply air was cooled and doubled in mass flow rate through the use of an ejector at the wing root. The blown ailerons could be drooped 20 deg to further increase the wing lift coefficient.

The WVU Circulation Control Technology Demonstrator Aircraft was completed in 1974. The flight tests were started on April 10, 1974, and have been described by the test pilot, Roberts, in Ref. 14. Further details on the aircraft's construction, design, and flight test were given by Loth et al. in Ref. 15. Although the aspect ratio of the aircraft was only 7.15, and only 58% of its span was equipped with a circulation control flap, its performance nearly equaled that of the two-dimensional model B wing tested at low Reynolds number in the wind tunnel. The flight test results for the CC wing performance can be summarized by the same empirical equation. With the flap stowed in the cruise configuration, the lift curve slope $\partial C_L/\partial\alpha = 5.1$. The value of $\partial C_L/\partial C_\mu$ was seriously affected by the propeller slipstream and could only be tested in power-off stalls which resulted in $\partial C_L/\partial C_\mu = 6.6/\sqrt{C_\mu}$. The maximum available lift coefficients at the onset of stall are given in Fig. 5. This demonstrates the high CC efficiency at very moderate blowing rates. For example, with propeller power off, the wing $C_{L_{max}}$ could be increased from 2.0 to 4.3 by turning the blowing air on and increasing C_μ from 0 to 0.12. Note that these values are based on the cruise wing area instead of the CC wing area. With flap out, the wing area is 12% larger than in cruise.

The forward folding and stowing of the flap proved to present no problems to the pilot. At large flap angles, the air velocity below the flap hinge is very low and the flap operation in this near stagnant air region is quite acceptable when done rapidly. In-flight rapid flap retraction from full out at $\beta = 0$ deg, turning through an angle β up to the 173-deg stowed position, took only 4 s. The in-flight flap deployment takes only 2.5 s and is noticed as a bump to the aircraft that is easily controllable. Flap transient data were obtained by a series of flap deployment increments, starting with the stowed flap cruise configuration. The stick force, elevator angle, and flap angle were measured at each increment while maintaining a constant flight speed of 130 k/h (70 knots). The results are given in Ref. 15. The maximum elevator stick force excursion was a push of 8.0 kg (16 lb) and resulted in a deployed flap out of trim conditions of 5 kg (10 lb) stick force.

The shortcomings of the model B wing flap design are as follows: The flap actuator air supply duct has to be located at the flap hinge line, and that restricts the location of the wing cavity in which the CC blowing tube is to be stored. In addition, the flap actuating torque and the wing drag with the flap in the vertical down position are high. These problems could be eliminated using the proposed CC stowed flap design shown in Fig. 6. Here, a conventional sliding Fowler flap is used either separately or in conjunction with the CC blowing tube. The tube can now be stored in a cavity at any convenient location in the wing. The CC blowing tube deployment will require little torque and create only minimal changes in drag and longitudinal trim. In the CC mode, the ejector suction could couple the blowing tube securely to the Fowler flap trailing edge. This new CC flap configuration is currently under investigation at WVU.

The STOL aircraft wing application of circulation control was further investigated by Englar at NSDRC. In June 1974, he proposed to modify a NAVY A6A aircraft to incorporate circulation control. Englar performed very extensive wind tunnel tests on the A6A wing (see Ref. 1). The wind tunnel test at a constant slot height ratio $h/c = 0.00118$ matches the previously given empirical equation rather well, with

$$\frac{\partial C_L}{\partial \alpha} = 5.1 \quad \text{and} \quad \frac{\partial C_L}{\partial C_\mu} = \frac{6.2}{\sqrt{C_\mu}}$$

The A6A aspect ratio is 5.31, and his test results correlate well with test data obtained with the flight tests of the WVU Circulation Control Technology Demonstrator Aircraft. The A6A wing modification was very difficult because an existing wing had to be used. Consequently, the cavity required to store the CC blowing tube for high-speed cruise could not be accommodated inside the existing wing structure. Thus the CC high lift modification had to be added to the wing as a permanent fixture. The very high temperature and pressure of the A6A jet engine bleed air required the use of titanium and steel. The flight test of this CC modified A6A aircraft was conducted by the contractor in 1979. The flight handling characteristics were analyzed very extensively and confirmed the potential of circulation control. The flight test results of the modified A6A were reported by Pugliese.[16]

The Effect of the Velocity Ratio V_j/V_∞

Normally the blowing power air supply comes from compressor bleed air of the main thrust jet engines. Most jet engines provide only high-pressure bleed air at more than 2 or 3 atm. The high pressure of the bleed air has the advantage that it minimizes the required air duct size. Jet engine bleed air test results by Hemmerly[17] on a J 52-P-8A engine have demonstrated that up to 16% of the engine mass flow rate is available as bleed air at pressures ranging from 3 to 13 atm. The engine thrust loss associated with engine bleed air is high. For example 5% bleed air results in 10% of engine thrust loss.

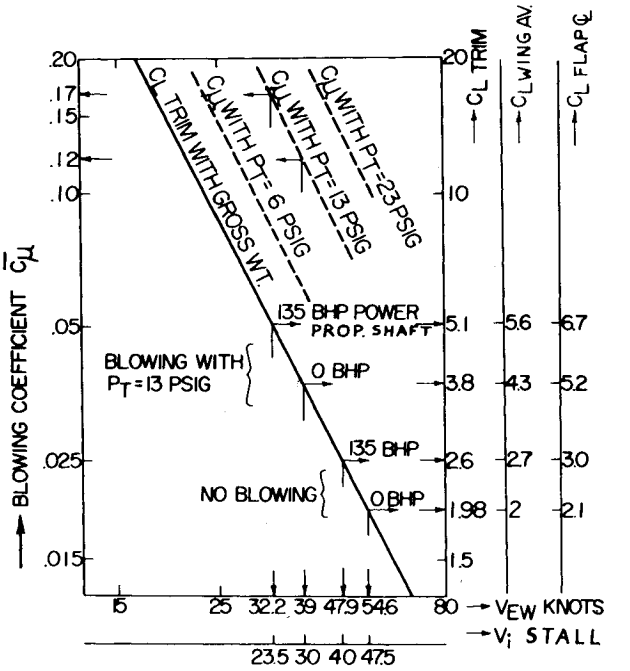

Fig. 5 WVU Technology Demonstrator Aircraft stall performance with and without propeller thrust power at various CC blowing pressures.

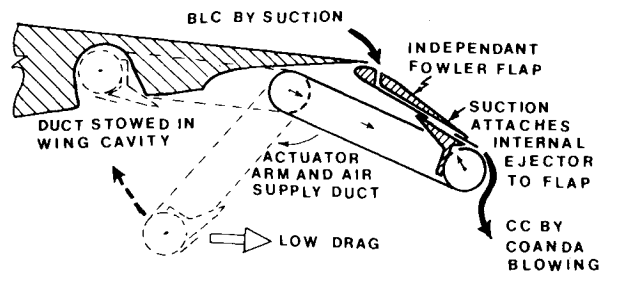

Fig. 6 Proposed low drag and low torque retraction of the CC round Coanda surface. The conventional Fowler flap can be used with or without CC blowing.

This bleed air can produce only one-third of this 10% thrust loss in the form of jet blowing momentum, $\dot{m}_j V_j$. Thus careful conservation of the jet blowing momentum must be practiced in the CC wing design. Any air bleed pressure above 2 atm results in a supersonic nozzle velocity V_n. Although one can achieve circulation control with a supersonic wall jet, such a jet loses a significant portion of its momentum to wall shear. Only the remaining jet momentum will be available to energize the Coanda surface boundary layer.

Englar[18] showed that with high-velocity ratios, the Coanda path length should be reduced by using a smaller trailing edge radius. His data, taken with a CC modified NASA supercritical airfoil, give a good insight in the effect of the velocity ratio on CC performance. Data from Fig. 7 in Ref. 18, showing C_L as a function of the blowing pressure ratio have been replotted as a function of ΔC_L and the velocity ratio V_j/V_∞ (see Fig. 7). At constant slot height h/c, the lift augmentation increases linearly with V_j/V_∞. The empirical curve fit

$$\Delta C_L = 40(h/c)^{0.64}(V_j/V_\infty - 1) \tag{5}$$

is in excellent agreement with all the data except at the smallest slot with $h/c = 0.0003$. This may be due to the widening of the slot with increasing pressure. The resulting optimization of V_j/V_∞ for maximum C_L, depends on the quantity that is held constant. This is shown in Fig. 8. If the slot height (h/c) is held constant, then ΔC_L increases linearly with V_j/V_∞. If the blowing volume flow rate $[(h/c)\cdot(V_j/V_\infty)]$ is held constant, then the rate of increase of ΔC_L with V_j/V_∞ will be reduced.

If the blowing momentum $[(h/2c)\cdot(V_j/V_\infty)^2 = C_\mu]$ is held constant, then ΔC_L increases up to $V_j/V_\infty = 4.57$ and decreases at higher values. If the blowing power $[(h/c)\cdot(V_j/V_\infty)^3 = C_\mu V_j/(2V_\infty)]$ is held constant, then ΔC_L increases up to $V_j/V_\infty = 2.08$ and decreases rapidly at higher V_j/V_∞. However, if the pressure and thus power loss inside the blowing air supply duct is included, then the optimum velocity ratio can be significantly higher.

If the available air supply is at a high pressure, then the required mass flow rate and thus the power can be minimized by employing an internal wall jet ejector. Such an ejector can reduce the velocity ratio by a factor of 2 and increase the momentum coefficient C_μ slightly. For example, the thrust augmenter analysis in Ref. 1, can be used to provide an insight into the relation between parameters such as A, V_j/V_n, $\dot{m}_j/\dot{m}_n$, and the momentum augmentation. The area ratio A is the ratio between the primary flow nozzle slot height and the ejector exit height, which is the wall jet slot thickness h. The von Kármán thrust augmenter analysis gives the mass flow ratio between the nozzle bleed airflow rate $\dot{m}_n$ and $\dot{m}_j$ as

$$\dot{m}_j/\dot{m}_n = \frac{V_j}{V_n}\frac{1}{A} \tag{6}$$

where

$$\frac{V_j}{V_n} = \frac{-A(1-2A)+\sqrt{2A-6A^2+6A^3-2A^4}}{1-2A+2A^2} \tag{7}$$

For $A = 0.25$, find $V_j/V_n = 0.535$ and $\dot{m}_j/\dot{m}_n = 2.14$. The entrained ejector mass flow rate $\dot{m}_s$ can provide boundary-layer control by suction and equals $\dot{m}_j - \dot{m}_n$. The momentum augmentation in this example is $C_{\mu j}/C_{\mu n} = 1.14$.

Applying such an ejector with an area ratio of 4 to the CC wing performance shown in Fig. 7 will result in the following improvement. Without the ejector, at $V_j/V_\infty = 12$ and $h/c = 0.0003$ results in $\Delta C_L = 2.45$. But by adding the ejector, the velocity ratio can be reduced to $V_j/V_\infty = 6.42$ and the slot height be increased to $h/c = 0.0012$. This raises ΔC_L to 2.93, or a 20% increase in performance.

The effect that the magnitude of V_j/V_∞, C_μ, and h/δ^* have on the jet momentum loss to wall shear, can easily be estimated. The Blasius flat plate turbulent boundary-layer (BL) analysis provides the equations for the BL displacement thickness δ^* and the wall shear friction coefficient C_f as a function of the Reynolds number. For STOL applications, the freestream velocity V_∞ can be as low as 30 m/s (100 ft/s) and the wing Reynolds number $Re_c = V_\infty c/\nu$ in the order of 2.5×10^6. By assuming the jet engine bleed air to be supplied by an isentropic compressor and duct, then after expansion to ambient pressure in an isentropic nozzle, its static temperature and density will return to ambient conditions. The resulting two-dimensional blowing coefficient can then be simplified to

$$C_\mu = \frac{\dot{m}_j V_j}{\tfrac{1}{2}\rho V_\infty^2 c} = 2\left(\frac{v}{c}\right)\left(\frac{V_j}{V_\infty}\right)^2 \tag{8}$$

With a typical circulation control momentum coefficient $C_\mu = 0.2$ and velocity ratio $V_j/V_\infty = 10$, the resulting slot height will be $h/c = 0.001$. The corresponding boundary-layer thickness for a flat plate of length c is

$$\delta/c = 0.37/R_{ec}^{0.2} = 0.02 \tag{9}$$

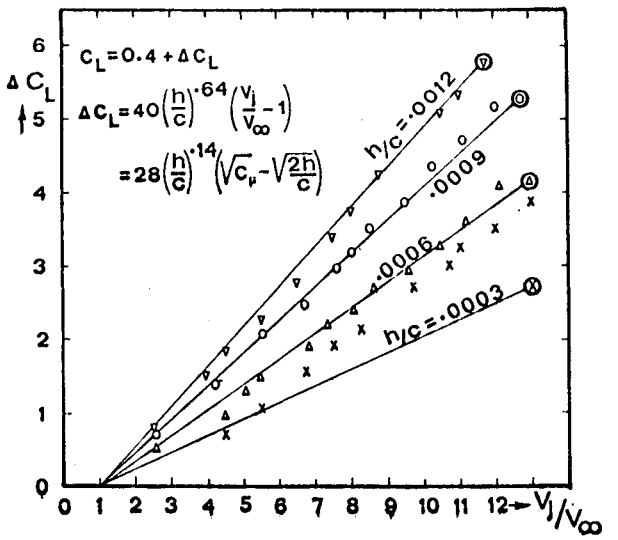

Fig. 7 Constant slot height data by Englar replotted as a function of the wall jet velocity ratio V_j/V_∞. (Data from Ref. 18).

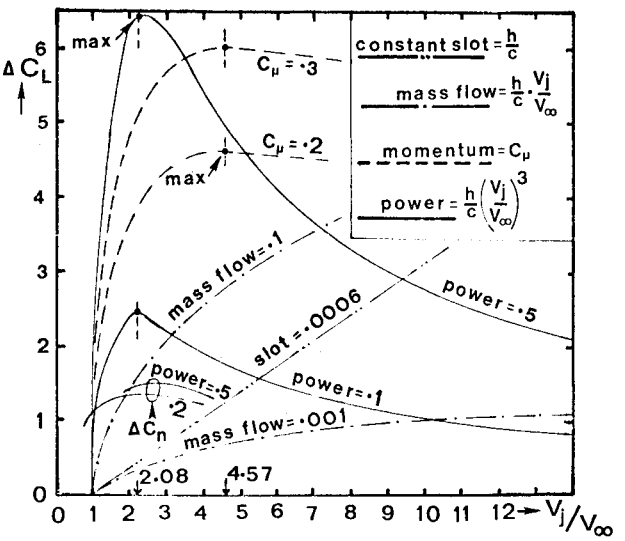

Fig. 8 Calculated curves of constant mass flow rate, blowing momentum, and blowing power showing the significance of the velocity ratio V_j/V_∞.

Or $\delta/h=20$ and h is only a small fraction of δ. A relatively thick wall jet enhances a rapid boundary-layer energization, prior to losing its momentum to wall shear. Assuming an average Coanda surface shear friction coefficient C_f over a distance equal the boundary-layer thickness gives

$$C_f=\frac{0.296}{Re_j^{0.2}}=\frac{0.296}{[(\delta/c)(V_j/V_\infty)Re_c]^{0.2}} \tag{10}$$

The above example gives $C_f=0.02$. Then the fraction of wall jet momentum lost to wall shear in that distance is

$$f=\frac{C_f \tfrac{1}{2}\rho V_j^2 \delta}{\dot{m}_j V_j}=\tfrac{1}{2}\left(\frac{\delta}{h}\right)C_f \tag{11}$$

For this example find $f=0.2$ and thus 20% of the wall jet momentum is lost to wall shear.

Increasing the velocity ratio to 14 would double the ratio δ/h to 40, have almost no effect on C_f but double the value of f, and then lose 40% of the wall jet momentum to shear. This wall shear loss difference demonstrates the advantages of using a subsonic wall jet. For STOL applications when dealing with a high-pressure CC air supply, one should reduce the wall jet velocity to subsonic speed with an internal ejector. However, if one cannot convert the rounded CC trailing edge in flight to a sharp, low drag configuration, one may have to resort to a small trailing edge radius and associated high-velocity thin jet.

The powerful numerical solutions presently available are ideally suited to compute the performance of CC STOL wings. The two-dimensional boundary-layer formation and the effects of boundary-layer removal by suction, wall jet entrainment, and Coanda flow separation can all be analyzed with the current state-of-the-art of viscous flow analysis. To maximize the computational efficiency it is necessary to separate the flowfield into distinct regions that match in pressure and velocities at their boundaries. The exterior potential flowfield is matched with a parabolic solution of the boundary-layer equations, as given by Keller and Cebeci.[19] In the neighborhood of the suction and blowing slot, the solution becomes elliptic in nature. An inviscid solution using the superposition of sinks and uniform flow can be used to account for the upstream effects of suction or blowing. The entrainment effects result in a slightly more favorable pressure gradient upstream of the slot, due to the flowfield curvature. A single suction slot does little to delay boundary-layer separation. But the removal of the boundary sublayer by the suction slot improves the shape factor and the Coanda turning of the wall jet.

The effect of V_j/V_∞ on the required blowing power for the prevention of stall in an adverse pressure gradient has been computed for a special case. A flat plate has been considered with an adverse pressure gradient, corresponding to a radial source flow-like velocity decrease. At the point of flow separation without blowing, a wall jet was positioned. By varying the slot height and the jet velocity V_j, the flow separation point can be delayed over a significant distance. To interpret these results in terms of ΔC_L and V_j/V_∞, one can compare this flowfield to the flow over the aft portion of a cusped trailing edge airfoil. The airfoil operates near $C_{L\max}$ if its boundary layer is at the point of separating at the trailing edge where $V=V_\infty$ and $p=p_\infty$. Then, using the pressure and velocity at the point of separation on the flat plate as reference values, one can plot a normal force coefficient ΔC_n as a function of V_j/V_∞. This is shown in Fig. 8 for various lines of constant blowing power $[(h/c)\cdot(V_j/V_\infty)^3]$. It clearly shows that ΔC_n peaks at velocity ratios between 2 and 3.0 just like the performance model based on Englar's data and shown in the same figure.

Conclusions

Circulation control by blowing over a rounded trailing surface is an efficient method of achieving STOL capability. The CC advantages of powerful direct lift control, roll control by differential blowing, and good visibility in a level approach attitude are very desirable STOL aircraft characteristics. The amount of blowing air supply required is small enough, and does not seriously reduce the available engine thrust. Transport aircraft can significantly reduce the runway length requirements by applying circulation control even with an auxilary compressed air powerplant. The application of an internal wall jet ejector can substantially improve the aerodynamics of the high lift airfoil. Both the BL shape factor improvement by suction and the increased jet mixing by thickening the Coanda wall jet ejector improve the CC performance. Structural advantages are the resulting flap cooling and the increase in the exposed exit slot height. Because most of the fuel used by the aircraft will be in the cruise configuration, optimizing the wing for efficient cruise is more important than for efficient STOL. The need for an in-flight conversion from the rounded trailing surface CC configuration, to a low drag sharp trailing edge cruise configuration, is essential for the commercial application of CC.

References

[1] Kohlman, D.L., *Introduction to V/STOL Airplanes,* Iowa State University Press, Ames, Iowa, 1981.

[2] Loth, J.L., "Some Aspects of STOL Aircraft Aerodynamics," SAE Paper 730328, Business Aircraft Meeting, Wichita Kansas, April 1973.

[3] Pfenninger, W., "Design Considerations of Propulsive Systems for Low Drag BLC Airplanes Cruising at High Subsonic Speeds," NOR-59-418, Northrop Co., Hawthorne, Calif., July 1959.

[4] Katzmayr, R., "Berichte der Aeromechanischen Versuganstalt," Wien Vol. 1, No. 57, 1928, see also NACA Technical Memo. 521, Sept. 1929.

[5] Spence, D.A., "The Lift of a Thin Jet Flapped Wing," *Proceedings of the Royal Society, Series A,* No. 238, 1956, pp. 46-68.

[6] McCormick, B.W., *Aerodynamics of V/STOL Flight,* Academic Press, New York, 1967.

[7] Wilson, J.D., Chandra, S., and Loth, J.L., "Thrust Augmented Wing Sections in Transition Flight," AIAA Paper 75-169, Jan. 1975.

[8] Bevilaqua, P.M., Cole, P.E., and Schum, E.F., "Progress toward a Theory of Jet Flap Thrust Recovery," AFOSR Final Contract Report NR80H-76, Rockwell International, Columbus, Ohio, 1980.

[9] Metral, A. and Zerner, F., "The Coanda Effect," *Publication Scientifiques et Technique du Ministere de l'Air,* No. 218, 1948.

[10] Davidson, I.M., "Aerofoil Boundary-Layer Control System," British Patent No. 913754, 1960.

[11] Kind, R.J. and Maull, D.J., "An Experimental Investigation of a Low-Speed Circulation Controlled Aerofoil," *Aeronautical Quarterly,* Vol. XIX, May 1968, pp. 170-182.

[12] Williams, R.M., "Some Research on Rotor Circulation Control," *Proceedings of the Third Cal/AVLABS Symposium,* Cornell-Aero. Lab, Buffalo, New York, Vol. 11, June 1969.

[13] Gibbs, E.H. and Ness, N., "Analysis of Circulation Controlled Airfoils," West Virginia University, Morgantown, W.Va., Aerospace Engineering TR-43, June 1975.

[14] Roberts, S.C., "WVU Circulation Controlled STOL Aircraft Flight Tests," West Virginia University, Morgantown, W.Va., Aerospace TR-42, July 1974.

[15] Loth, J.L., Fanucci, J.B., and Roberts, S.C., "Flight Performance of a Circulation Controlled STOL Aircraft," *Journal of Aircraft,* Vol. 13, March 1976, pp. 169-173.

[16] Pugliese, A.J. and Englar, R.J., "Flight Testing the Circulation Controlled Wing," AIAA Paper 79-1791, New York, N.Y., Aug. 20, 1979; see also *Aviation Week and Space Technology,* March 19, 1979.

[17] Hemmerly, R.A., "An Investigation of the Performance of a J52-P-8A Engine Operation under the Influence of High Bleed Flow Extraction Rates," DT NSRDC ASED-387, Aug. 1977.

[18] Englar, R.J., "Low-Speed Aerodynamic Characteristics of a Small Fixed Trailing Edge Circulation Control Wing Configuration," DTNSRDC/ASED-81/08, NSRDC, Bethesda, Md., March 1981.

[19] Keller, H.B. and Cebeci, T., "Accurate Numerical Methods for Boundary Layer Flows, I: Two Dimensional Turbulent Flows," *AIAA Journal,* Vol. 10, Sept. 1972, pp. 1193-1199.